

Article

DFT Investigation of the Effects of Coexisting Cations and Complexing Reagents on Ni(II) Adsorption by a Polyvinylidene Fluoride-Type Chelating Membrane Bearing Poly(Amino Phosphonic Acid) Groups

Xiuli Wang ¹, Laizhou Song ^{1,*}, Caili Tian ², Jun He ¹, Shuaijie Wang ¹, Jinbo Wang ¹ and Chunyu Li ¹

¹ College of Environmental and Chemical Engineering, Yanshan University, Qinhuangdao 066004, China; xlwang7904@ysu.edu.cn (X.W.); hejun@ysu.edu.cn (J.H.); wangshuaijie@ysu.edu.cn (S.W.); wangjinbo123@163.com (J.W.); lcy1002@yeah.net (C.L.)

² Institute of Energy Resources, Hebei Academy of Sciences, Shijiazhuang 050081, China; tcl1998@126.com

* Correspondence: songlz@ysu.edu.cn; Tel.: +86-335-8387741; Fax: +86-335-8061569

Academic Editor: Peng Cao

Received: 29 November 2016; Accepted: 10 February 2017; Published: 17 February 2017

Abstract: A polyvinylidene fluoride (PVDF)-type chelating membrane bearing poly(amino phosphonic acid) groups, denoted as ethylenediamine tetra(methylene phosphonic acid) (EDTMPA)-tetrabutyl orthotitanate (TBOT)/PVDF, was employed to remove Ni(II) from the aqueous solution. The effects of coexisting Ca(II), Pb(II), citrate, nitrilotriacetic acid (NTA) and ethylenediaminetetraacetic acid (EDTA) on the Ni(II) adsorption by this chelating membrane were revealed using density functional theory (DFT) calculations. Pb(II) showed a more detrimental effect than Ca(II) on the Ni(II) uptake; EDTA interfered with the capture of Ni(II) more remarkably than citrate and NTA. The results derived from DFT calculations were consistent with the experimental data. Ni(II) and Pb(II) showed more excellent affinity to the EDTMPA-TBOT/PVDF membrane than Ca(II). The stabilities between Ni(II) and the [EDTMPA-TBOT]⁷⁻ chelating ligand of the membrane and those between Ni(II) and the three aforementioned complexing reagents followed the sequence: [Ni(II)-(EDTMPA-TBOT)]⁵⁻ > Ni(II)-EDTA > Ni(II)-NTA > Ni(II)-citrate. The complexation between Ni(II) and the chelating membrane was prominent with the presence of citrate, NTA and EDTA.

Keywords: nickel ion; polyvinylidene fluoride-type chelating membrane; adsorption; density functional theory; coexisting cation; complexing reagent

1. Introduction

The heavy metal pollution for water bodies has been a critical environmental problem of global concern. Being one of the most toxic metals, the nickel ion with non-biodegradable characteristics has been validated as a carcinogen; it easily accumulates in organisms, thereby resulting in toxicities to ecological systems and human beings' health [1–3]. Discharged effluents containing Ni(II) mainly come from the mining of nickel ores, metallurgy, welding, nickel electroless and electroplating. The discharged concentration of total nickel in China is strictly limited within 0.1 mg/L according to the published Chinese regulation of “Emission standard of pollutants for electroplating (GB 21900-2008)” [4]. Thus, the concentration of discharged Ni(II) should meet the requirement mentioned above. In effluents derived from metallurgy, circuit board manufacturing and nickel electroless plating industries, besides nickel ions, other substances, such as Ca(II), Pb(II), citrate, nitrilotriacetic acid (NTA) and ethylenediaminetetraacetic acid (EDTA) may be coexistent with Ni(II). Undoubtedly, the coexisting cations and organic reagents mentioned above can retard the removal

of Ni(II). From this viewpoint, the exploitation of effective techniques with an excellent disposal performance for Ni(II) is thus of great significance for the removal of this metal with the presence of coexisting substances.

Numerous techniques are feasible for removing Ni(II) from wastewater to guarantee that this metal pollutant is discharged with a concentration smaller than the required value of 0.1 mg/L. Techniques of chemical precipitation, biological treatment, ion exchange, solvent extraction, flotation, electrocoagulation, adsorption and membrane separation processes [5–14] have been attempted so far. Among the above processes employed to capture Ni(II), the membrane separation technique deserves to be considered because of its merits of higher efficiency, inconspicuous pressure drop and shorter axial-diffusion path [15,16]. As for the membrane techniques of electrodialysis, liquid membrane extraction, nanofiltration, reverse osmosis and polymer-enhanced ultrafiltration [14,17–20], the drawbacks of high costs and fussy pretreatments of these membrane techniques restrain their wide applications. On the other hand, compared with the membrane techniques mentioned above, the microfiltration and ultrafiltration may be more applicable for removing Ni(II), with respect to their fascinating characteristics of high permeation flux, inexpensive investment and lacking strict pretreatments. Generally, the two aforesaid conventional membrane techniques cannot be of benefit for the removal of the dissolvable Ni(II). In light of the adsorption treatment of heavy metals by the chelating resin, the chelating groups with a high affinity to metals incorporated into the microfiltration (or ultrafiltration) membrane matrix will be helpful in the Ni(II) removal. Various chelating groups, including pentaethylenhexamine, polyacrylic acid, ethylamine ligand, polyethylene imine, hyperbranched poly(amidoamine), NTA, diethylenetriaminepentaacetic acid (DTPA), ethylenediamine tetra(methylene phosphonic acid) (EDTMPA) and EDTA, can be suitable for the candidates incorporated into the membrane framework [21–30]. Among them, in our previous study [15,28], the DTPA group blended into the PVDF-type chelating membrane has been attested for the capture of Cu(II) and Ni(II). Similar to the DTPA, amino phosphonic acid, such as EDTMPA, shows an excellent affinity to metal pollutants. Thus, the enhancement in the Ni(II) uptake from the solution for both microfiltration and ultrafiltration membranes by the incorporation of EDTMPA groups can be considered.

In general, most adsorption studies have focused on the experiment scale. There is no doubt that the adsorption experiment can be helpful in the description of the adsorption kinetics and thermodynamics, but more details in the immanent interaction between the solute and the absorbent will not be elucidated comprehensively. The density functional theory (DFT) simulation, identified as a valuable supplement of the experiments [31–34], has been applicable for revealing various chemical problems; of course, adsorption studies are involved [15,35–39]. Whereas insufficient efforts related to the DFT simulation have paid attention to the Ni(II) adsorption by the PVDF-type membrane bearing the EDTMPA groups, herein, we confirm that this research will provide a proposal for the preparation of novel membranes and the removal of heavy metals.

In this research, a PVDF-type chelating membrane bearing the EDTMPA group was employed to remove Ni(II) from the aqueous solution in the presence of Pb(II) and Ca(II) cations and citrate, NTA and EDTA complexing reagents. The density functional theory (DFT) simulation was employed to elucidate the Ni(II) adsorption characteristics of the chelating membrane and to reveal the effects of the five aforementioned coexisting substances on the Ni(II) uptake. In this work, three DFT descriptors, i.e., chemical potential (μ), hardness (η) and global electrophilicity (ω), were calculated to explore the chemical reactivity of the EDTMPA group of the chelating membrane, Ni(II) and the coexisting Pb(II), Ca(II), citrate, NTA and EDTA. Furthermore, the charge transfer (ΔN), the adsorption energies (ΔE_{ads}) and the Gibbs free energies of adsorption (ΔG_{ads}) between the chelating membrane and three metal ions and those between Ni(II) and the three above complexing reagents were calculated.

2. Materials and Methods

2.1. Materials

PVDF powders were purchased from Chen Guang Co., Ltd., (Chengdu, China); the average molecular weight of this polymer is 400,000. Polyvinylpyrrolidone (PVP), dimethyl sulfoxide (DMSO), EDTMPA, absolute ethanol (C_2H_5OH) and tetrabutyl orthotitanate (TBOT) were applied to prepare the chelating membrane. Analytical-grade $Ni(NO_3)_2 \cdot 6H_2O$, $Pb(NO_3)_2$, $CaCl_2 \cdot 4H_2O$, citrate, NTA, ethylenediaminetetraacetic acid disodium salt ($EDTA-2Na^+$) and NaOH employed in this experiment were supplied by Jingchun Scientific Co., Ltd., (Shanghai, China). Without further purification, all reagents were used as received.

2.2. Preparation of the Chelating Membrane

At first, 2.0 g of EDTMPA were dissolved in 40 mL of ethanol aqueous solution, and the volume ratio between C_2H_5OH and H_2O was 1:3; the pH of the solution was adjusted to 6.0 by 5 mol/L of NaOH solution. After that, 4.7 mL of TBOT were dropwise added into this solution, and this solution was magnetically stirred at room temperature for 24 h to obtain a microparticle-containing solution; and then, the microparticle was separated by centrifugation at 3000 rpm for 10 min. The obtained microparticle (labeled as EDTMPA-TBOT) was centrifugally washed three times using absolute ethanol and DMSO. Afterward, 4.8 g of PVDF and 0.53 g of PVP were dissolved in 25 mL of DMSO at 353 K, and the fabricated EDTMPA-TBOT powder was subsequently added into this solution. At this temperature, the solution was stirred for 6 h. Lastly, a phase inversion technique was employed to prepare the PVDF-based chelating membrane [15,28]. The fabricated membrane (EDTMPA-TBOT/PVDF) was cleaned by deionized water and then kept for characterizations and adsorption tests.

2.3. Characterization of the Membrane

The morphology of the chelating membrane was characterized by an FE-SEM (SUPRA55, Zeiss, Jena, Germany) with an accelerating voltage of 5 kV; the compositions of the surface membrane were determined with an X-Max EDS (Oxford Instruments, Oxford, UK.) attached to the scanning microscope. FTIR spectra of the EDTMPA-TBOT chelating group before and after the Ni(II) uptake were examined using an E55 + FRA106 FTIR spectrometer (Bruker, Karlsruhe, Germany). In addition, the water permeability method was applied to characterize the mean pore size of the chelating membrane [40].

2.4. Adsorption Experiments

In 200-mL solutions containing 1.0 mmol/L of Ni(II) with an ~0.2 g addition of the chelating membrane, batch adsorption experiments for Ni(II) adsorption by the membrane were carried out at the temperature of 298 K. The pH of this solution was adjusted to 5.4 by the buffer containing 0.3 mol/L acetic acid and 0.2 mol/L sodium acetate. The effects of coexisting Ca(II), Pb(II), citrate, NTA and EDTA with different concentration (0–5 mmol/L) on the Ni(II) uptake were also evaluated.

2.5. Computational Details

All DFT calculations were implemented by the Materials Studio DMol³ code [39,41] with Version of 7.0, which was provided by Accelrys Inc., (San Diego, CA, USA). In this research, the generalized gradient approximation (GGA) level with the spin unrestricted approach, double numerical plus polarization functions (DNP) and Becke exchange functional in conjunction with the Lee–Yang–Parr correlation functional (BLYP) were employed to optimize the structures. In order to accelerate self-consistent field convergence, Pulay's direct inversion in the iterative subspace (DIIS) technique and the small electron thermal smearing with a value of 0.005 Ha were applied. To obtain the

geometrical and energetic parameters, Mulliken population analyses and frequency were calculated. A continuum solvation model (COSMO) with the dielectric constant of water as 78.54 was employed considering the aqueous adsorption. In regard to the effect of weak interactions (such as hydrogen bond and Van der Waals force), the Tkatchenko–Scheffler (TS) method for DFT dispersion correction was also used.

3. Results and Discussion

3.1. Characterization of the Chelating Membrane

3.1.1. Analyses of FE-SEM and EDS

The morphologies of the fabricated EDTMPA-TBOT/PVDF chelating membrane were observed; surface and sectional morphologies of the membrane are shown in Figure 1a,b. For the surface morphology (Figure 1a), the uniform microporous structure can be identified. The presence of micropores with an average size of 0.25 μm will be helpful for the solution permeating through the membrane. In terms of the sectional morphology of the membrane, as shown by Figure 1b, the finger-like pores near the surface layer (labeled by a circle) are observed, and the sponge-type porous structures (described by a rectangle) can be found in the inner side of the membrane.

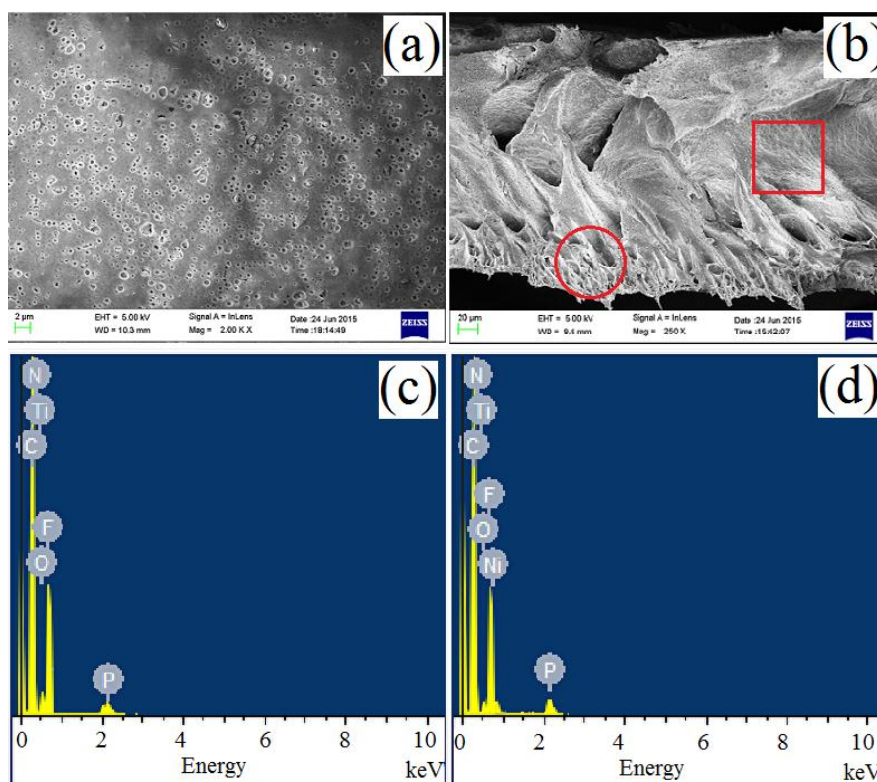


Figure 1. FE-SEM pictures and the EDS spectra of the ethylenediamine tetra(methylene phosphonic acid) (EDTMPA)-tetrabutyl orthotitanate (TBOT)/PVDF membrane: (a) surface morphology; (b) sectional morphology; (c) EDS before Ni(II) adsorption; (d) EDS after Ni(II) adsorption.

EDS spectra before the Ni(II) adsorption (Figure 1c) and after the Ni(II) adsorption by the chelating membrane (Figure 1d) were examined. Before the Ni(II) adsorption, as demonstrated by Figure 1c, besides the elements of carbon and fluorine, the elements of nitrogen, titanium, oxygen and phosphorus are detected, which indicates that the EDTMPA-TBOT groups were incorporated into the PVDF membrane matrix. After the Ni(II) uptake, by the comparison results of Figure 1c,d, the nickel element is detected, thereby suggesting the capture of Ni(II) by the chelating membrane.

3.1.2. FTIR Spectra

The availability of Ni(II) adsorption by the EDTMPA-TBOT/PVDF chelating membrane was also validated by FTIR analysis (Figure 2). Before and after Ni(II) adsorption (Figure 2a), for the FTIR spectra of the EDTMPA-TBOT/PVDF chelating membrane, in contrast with that of the virgin PVDF membrane, peaks at 890–1400 cm^{-1} show obvious changes, which can be attributed to the existence of the phosphonic acid groups of the EDTMPA-TBOT ligand. Herein, with and without the uptake of Ni(II), the difference in the FTIR spectra of the chelating membrane is inconspicuous; this may be assigned to the disturbance of PVDF chains. Thus, the FTIR spectra of the pure EDTMPA and the EDTMPA-TBOT powder before and after Ni(II) adsorption (Figure 2b) were also measured to eliminate this disturbance. The peaks appearing at 957 and 1007 cm^{-1} can be ascribed to the asymmetric stretching vibration of P–OH groups; other peaks located at 1100–1270 cm^{-1} are attributed to P=O stretching vibration [42,43]. The broad peak at 1670 cm^{-1} can be identified as the plane bending of the hydroxyl group in the phosphonic acid group [44]. Peaks at 1322 and 1435 cm^{-1} can be assigned to the stretching vibration of the C–N and P–C groups. For the spectrum of EDTMPA-TBOT powder, the characteristic peaks related to the phosphonic acid group (900–1270 cm^{-1}) divided into two peaks (1030 and 1150 cm^{-1}), indicating the formation of P–O–Ti bond [29]. The broad peak at 1670 cm^{-1} becomes sharp and shifts to 1650 cm^{-1} ; this can be due to the interaction between the TBOT and EDTMPA molecules and thereby suggesting the formation of the P–O–Ti bond.

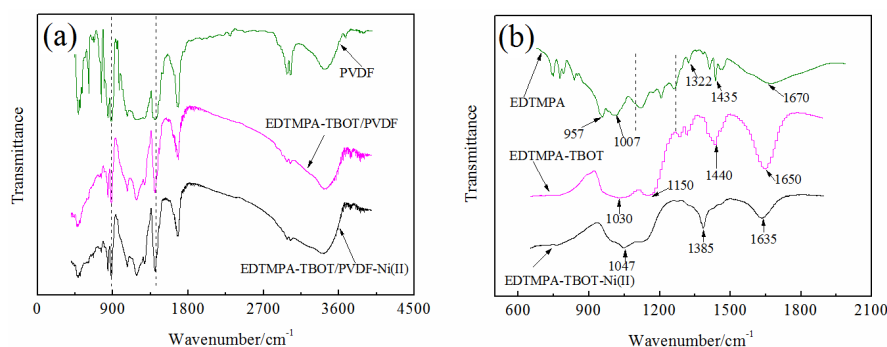


Figure 2. FTIR spectra: (a) the virgin PVDF membrane and the EDTMPA-TBOT/PVDF chelating membrane before and after Ni(II) adsorption; (b) the virgin EDTMPA and the EDTMPA-TBOT powder before and after Ni(II) adsorption.

For the spectrum after the Ni(II) adsorption compared with that before the Ni(II) adsorption, the peak at 1030 cm^{-1} shifts to 1047 cm^{-1} , and the intensity of this peak also slightly increases. The intensity of the peak at 1150 cm^{-1} related to the P=O stretching decreases, inferring the formation of the P–O–Ni(II) complexing bond. The peak at 1322 cm^{-1} in correlation with the C–N group almost completely disappears, and the formation of the N–Ni(II) bond can be validated [28]. In addition, the decrease in intensity for the peak at 1650 cm^{-1} accompanied by a negative shift of 15 cm^{-1} may be due to the fact that Ni(II) is complexed by the O–H group of the EDTMPA molecule [15,45].

3.2. Effects of Coexisting Cations

The coexisting Ca(II) and Pb(II) can hinder the Ni(II) adsorption. Ni(II) uptakes of the EDTMPA-TBOT/PVDF membrane in the presence of these two cations were measured to elucidate their interferences. Ni(II) uptakes of the membrane reduce with Ca(II) and Pb(II) concentrations increasing from 0 to 5 mmol/L (Figure 3); these two coexisting cations show an interferential effect on the uptake of Ni(II) because they compete with Ni(II) for occupying the active sites of the membrane. As Ca(II) and Pb(II) coexist with Ni(II) at the concentration of 1 mmol/L, Ni(II) uptake of the membrane decreases by 35% and 83%. Based on this result, it can be inferred that Pb(II) exhibits a more conspicuously detrimental effect than Ca(II) on the Ni(II) adsorption.

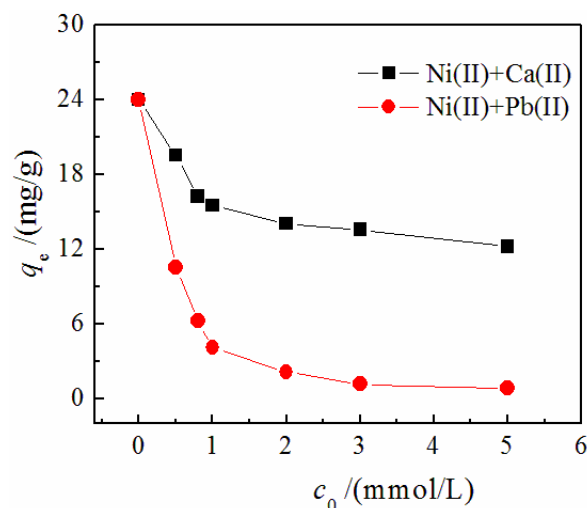


Figure 3. Effect of the coexistent cations on Ni(II) adsorption. $c_0(\text{Ni(II)}) = 1.0$ mmol/L; t : 360 min; membrane amount: ~ 0.2 g; T : 298 K; pH: 5.4.

3.3. Effects of Coexisting Complexing Reagents

The influences of citrate, NTA and EDTA coexisting with concentrations from 0 to 5 mmol/L on Ni(II) uptakes of the chelating membrane were studied, and the results are depicted in Figure 4. As the concentration of the three complexing reagents increases, the Ni(II) uptake of the chelating membrane decreases. This can be explained by the fact that most nickel ions are complexed with the increasing concentration of these three complexing reagents, and the complexed form of Ni(II) retards this metal uptake. As citrate, NTA and EDTA coexisted at a concentration of 1 mmol/L, the Ni(II) uptake of the membrane decreases by 26%, 53% and 73%, respectively. Thus, it can be concluded that the interferences of these three complexing reagents follow the order of citrate < NTA < EDTA. Although the disturbance of coexisting cations and complexing reagents is validated, the chelating membrane still exhibits the ability of Ni(II) capture, manifesting its potential application for removing Ni(II) from aqueous solutions.

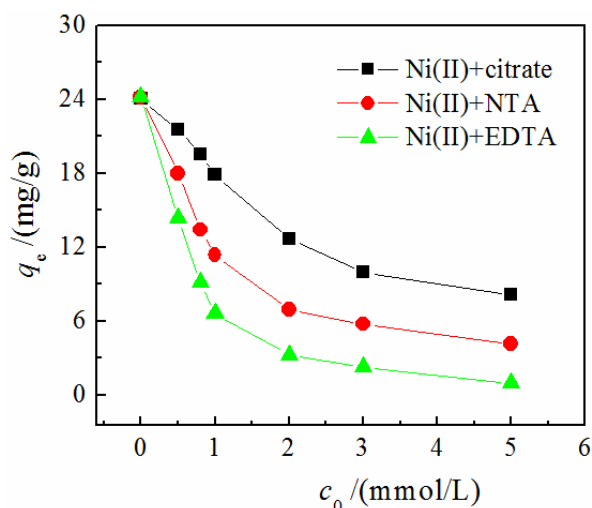


Figure 4. Effect of the coexistent complexing reagents on Ni(II) adsorption. $c_0(\text{Ni(II)}) = 1.0$ mmol/L; t : 360 min; membrane amount: ~ 0.2 g; T : 298 K; pH: 5.4.

3.4. DFT Simulations

3.4.1. Structure Analysis of the EDTMPA-TBOT Ligand

The optimized structure of the EDTMPA-TBOT ligand is given in Figure 5. Considering the difference of pH in the aqueous solution, the EDTMPA-TBOT ligand will exist in the forms of $[H_n(EDTMPA-TBOT)]^{(7-n)-}$ ($n = 0-7$). The free HySS2009 software (Protonic software, Leeds, UK) was employed to identify the species of the EDTMPA-TBOT ligand at different pH. The simulated existing forms of the EDTMPA-TBOT complexes are shown in Figure 6. As shown in Figure 6, at pH = 5.4, the EDTMPA-TBOT complexing ligand will be mainly in the form of $[EDTMPA-TBOT]^{7-}$. In addition, in view of the results of DFT calculation (not shown here), citrate, NTA and EDTA suitable for the capture of Ni(II) will exist in the forms of $[H_2Cit]^-$, $[H_2NTA]^-$ and $[H_2EDTA]^{2-}$, respectively. Hence, $[EDTMPA-TBOT]^{7-}$ ligand, $[H_2Cit]^-$, $[H_2NTA]^-$ and $[H_2EDTA]^{2-}$ were adopted as the computed geometries. The optimized structures of $[EDTMPA-TBOT]^{7-}$ ligand, $[H_2Cit]^-$, $[H_2NTA]^-$ and $[H_2EDTA]^{2-}$ are reported in Figure 7. In addition, the structures for Ni(II), Ca(II) and Pb(II) ions in the forms of $[Ni(II)(H_2O)_6]^{2+}$, $[Pb(II)(H_2O)_2]^{2+}$ and $[Ca(II)(H_2O)_8]^{2+}$ were employed [39,46].

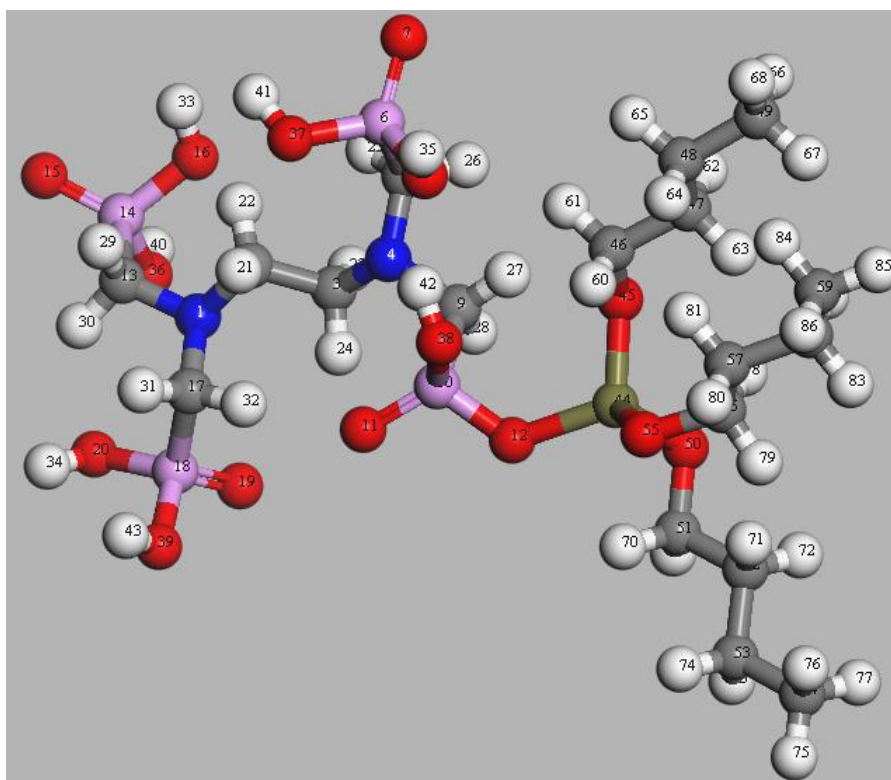


Figure 5. Optimized structure of EDTMPA-TBOT ligand with the numbered atoms: numbered atoms are denoted as follows: 21–35, 40–43, 60–86, hydrogen; 2, 3, 5, 9, 13, 17, 46–49, 56–59, 51–54, carbon; 7, 8, 11, 12, 15, 16, 19, 20, 36–39, 45, 50, 55, oxygen; 1, 4, nitrogen; 6, 10, 14, 18, phosphorus; 44, titanium.

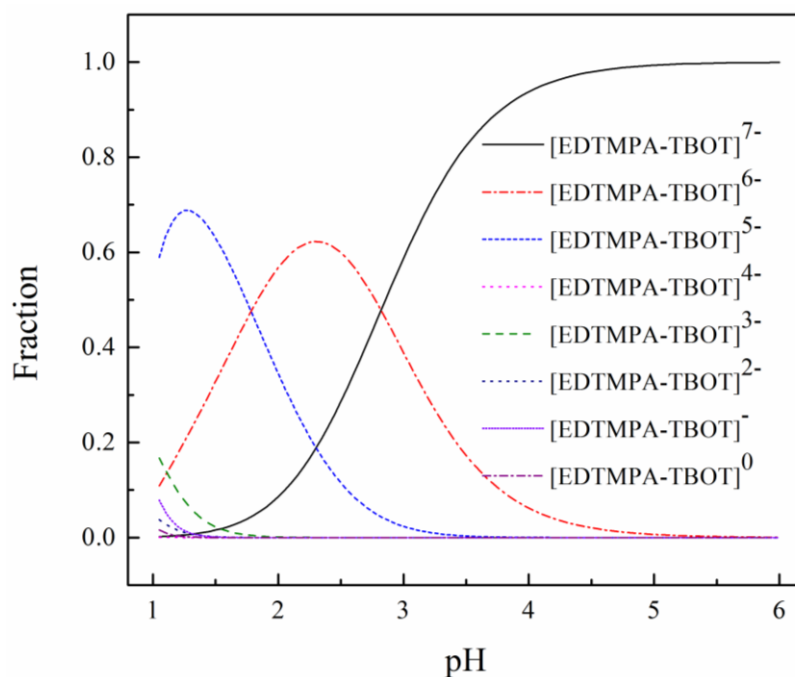


Figure 6. Distribution of the species for the EDTMPA-TBOT ligand as a function of pH by HySS2009.

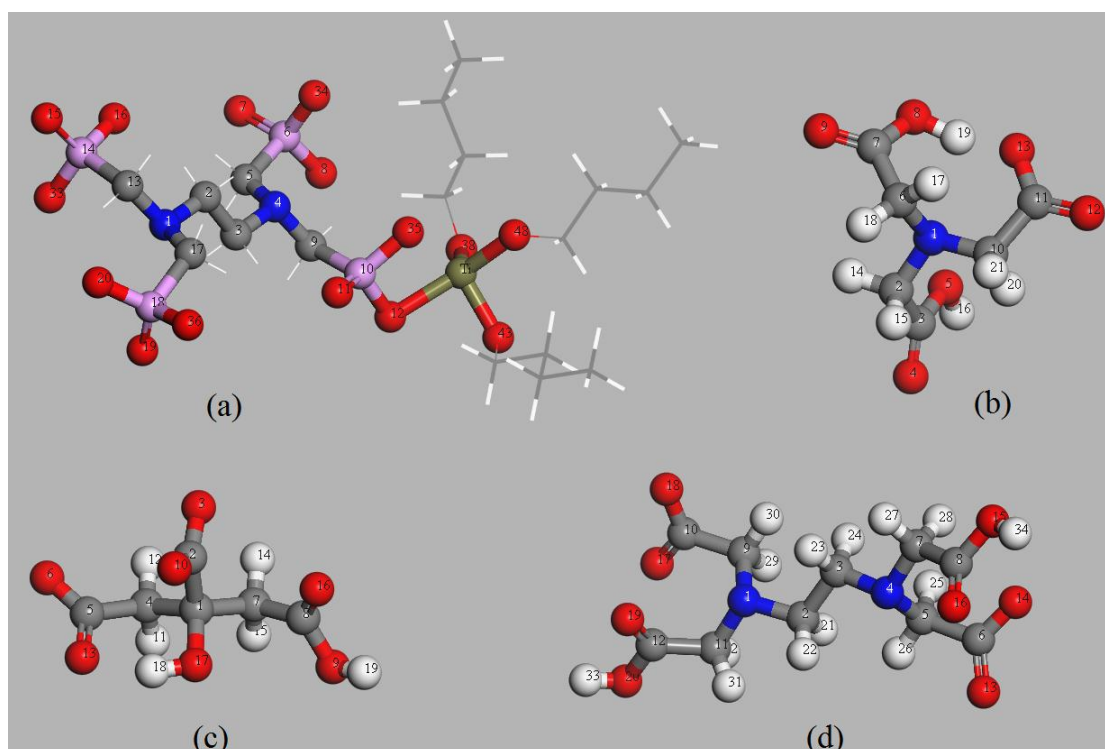


Figure 7. Optimized structures of the $[\text{EDTMPA-TBOT}]^{7-}$ ligand, $[\text{H}_2\text{NTA}]^-$, $[\text{H}_2\text{Cit}]^-$ and $[\text{H}_2\text{EDTA}]^{2-}$ with the numbered atoms: numbered atoms are denoted as follows: (a) $[\text{EDTMPA-TBOT}]^{7-}$ ligand (2, 3, 5, 9, 13, 17, carbon; 7, 8, 11, 12, 15, 16, 19, 20, 33–36, 38, 43, 48, oxygen; 1, 4, nitrogen; 6, 10, 14, 18, phosphorus); (b) $[\text{H}_2\text{NTA}]^-$ (14–21, hydrogen; 2, 3, 6, 7, 10, 11, carbon; 4, 5, 8, 9, 12, 13, oxygen; 1, nitrogen); (c) $[\text{H}_2\text{Cit}]^-$ (11, 12, 14, 15, 18, 19, hydrogen; 1, 2, 4, 5, 7, 8, carbon; 3, 6, 9, 10, 13, 16, 17, oxygen); (d) $[\text{H}_2\text{EDTA}]^{2-}$ (21–34, hydrogen; 2, 3, 5–12, carbon; 13–20, oxygen; 1, 4, nitrogen). NTA, nitrilotriacetic acid.

3.4.2. The Chemical Reactivity Descriptors

Energies of the highest occupied molecular orbital (HOMO), lowest unoccupied molecular orbital (LUMO) and the band gaps ($\Delta E_{\text{LUMO-HOMO}}$) of $[\text{EDTMPA-TBOT}]^{7-}$, $[\text{Ni(II)(H}_2\text{O)}_6]^{2+}$, $[\text{Pb(II)(H}_2\text{O)}_2]^{2+}$, $[\text{Ca(II)(H}_2\text{O)}_8]^{2+}$, $[\text{H}_2\text{Cit}]^-$, $[\text{H}_2\text{NTA}]^-$ and $[\text{H}_2\text{EDTA}]^{2-}$ were calculated, and the values are listed in Table 1. Of all of the reactants, the HOMO energy of $[\text{EDTMPA-TBOT}]^{7-}$ is the highest, and the LUMO energy of $[\text{Ni(II)(H}_2\text{O)}_6]^{2+}$ is the lowest, except $[\text{Pb(II)(H}_2\text{O)}_2]^{2+}$. In this sense, it can be confirmed that Ni(II) and the $[\text{EDTMPA-TBOT}]^{7-}$ ligand show the most noticeable tendencies for accepting electrons and donating electrons than other reactants. Furthermore, $[\text{EDTMPA-TBOT}]^{7-}$ and $[\text{Ni(II)(H}_2\text{O)}_6]^{2+}$ have smaller $\Delta E_{\text{LUMO-HOMO}}$ than other species, indicating that the $[\text{EDTMPA-TBOT}]^{7-}$ ligand and Ni(II) have remarkably nucleophilic and electrophilic characteristics, respectively. In addition, the E_{LUMO} of $[\text{Ni(II)(H}_2\text{O)}_6]^{2+}$ and $[\text{Pb(II)(H}_2\text{O)}_2]^{2+}$ are lower than the E_{HOMO} of the $[\text{EDTMPA-TBOT}]^{7-}$ ligand, suggesting that the chelating interaction between the $[\text{EDTMPA-TBOT}]^{7-}$ ligand and Ni(II) and that between the $[\text{EDTMPA-TBOT}]^{7-}$ ligand and Pb(II) take place easily. In other words, the EDTMPA-TBOT/PVDF chelating membrane shows excellent affinities to Ni(II) and Pb(II). The energy difference in the E_{LUMO} of Ni(II) and the E_{HOMO} of three complexing reagents follows the trend: $\Delta E(E_{\text{LUMO}}(\text{Ni(II)})-E_{\text{HOMO}}(\text{EDTA})) < \Delta E(E_{\text{LUMO}}(\text{Ni(II)})-E_{\text{HOMO}}(\text{NTA})) < \Delta E(E_{\text{LUMO}}(\text{Ni(II)})-E_{\text{HOMO}}(\text{citrate}))$, indicating that the interference of EDTA on Ni(II) adsorption is more remarkable than those of citrate and NTA.

The chemical reactivity descriptors of chemical potential (μ), global hardness (η) and electrophilicity (ω) can be calculated by Equations (1)–(3) [15,47].

$$\mu = \frac{(E_{\text{HOMO}} + E_{\text{LUMO}})}{2} \quad (1)$$

$$\eta = \frac{(E_{\text{LUMO}} - E_{\text{HOMO}})}{2} \quad (2)$$

$$\omega = \frac{\mu^2}{2\eta} \quad (3)$$

The chemical reactivity descriptors of the seven aforementioned reactants were calculated and summarized in Table 1. Values of μ for $[\text{Ni(II)(H}_2\text{O)}_6]^{2+}$, $[\text{Pb(II)(H}_2\text{O)}_2]^{2+}$ and $[\text{Ca(II)(H}_2\text{O)}_8]^{2+}$ are more negative than those of the $[\text{EDTMPA-TBOT}]^{7-}$ ligand, $[\text{H}_2\text{Cit}]^-$, $[\text{H}_2\text{NTA}]^-$ and $[\text{H}_2\text{EDTA}]^{2-}$. Therefore, Ni(II), Pb(II) and Ca(II) serve as electrophiles, while the $[\text{EDTMPA-TBOT}]^{7-}$ ligand and the three complexing reagents act as nucleophiles. Among the three electrophiles, the electronegativity ($\chi = -\mu$) shows a descending order of $[\text{Pb(II)(H}_2\text{O)}_2]^{2+} > [\text{Ni(II)(H}_2\text{O)}_6]^{2+} > [\text{Ca(II)(H}_2\text{O)}_8]^{2+}$. Compared with Ni(II) and Ca(II), Pb(II) can more easily obtain the electrons from the $[\text{EDTMPA-TBOT}]^{7-}$ ligand. However, for Ni(II), Pb(II) and Ca(II), the calculated values of η and ω are inconsistent with the order of χ , and this is also in contradiction with the experimental result. It can be inferred that the above-mentioned three cations may show a different electrophilic behavior in other reacting processes.

The χ value of the four above nucleophiles increases in the order of $[\text{EDTMPA-TBOT}]^{7-} < [\text{H}_2\text{EDTA}]^{2-} < [\text{H}_2\text{NTA}]^- < [\text{H}_2\text{Cit}]^-$, revealing that the $[\text{EDTMPA-TBOT}]^{7-}$ ligand owns a stronger nucleophilic ability than the other three complexing reagents. Moreover, the results of the analysis on the η and ω value of the $[\text{EDTMPA-TBOT}]^{7-}$ ligand and three complexing reagents are in accordance with that of χ . Thus, it indicates that the Ni(II) uptake of the EDTMPA-TBOT/PVDF chelating membrane plays a dominant role in the adsorption process with the presence of citrate, NTA and EDTA. Furthermore, it can be deduced that the interference of EDTA on Ni(II) adsorption is higher than those of citrate and NTA.

Table 1. Calculated E_{HOMO} , E_{LUMO} , $\Delta E_{\text{LUMO-HOMO}}$, μ , η and ω in Hatree for the [EDTMPA-TBOT] $^{7-}$ ligand, Ni(II), the coexistent cations and complexing reagents.

Chemical Species	$E_{\text{HOMO}}/\text{Ha}$	$E_{\text{LUMO}}/\text{Ha}$	$\Delta E_{\text{LUMO-HOMO}}/\text{Ha}$	μ/Ha	η/Ha	ω/Ha
[EDTMPA-TBOT] $^{7-}$	-0.1298	-0.0650	0.0648	-0.0974	0.0324	0.1464
[Ni(II)(H ₂ O) ₆] $^{2+}$	-0.2593	-0.1401	0.1192	-0.1997	0.0596	0.3346
[Pb(II)(H ₂ O) ₂] $^{2+}$	-0.3387	-0.1459	0.1928	-0.2423	0.0964	0.3045
[Ca(II)(H ₂ O) ₈] $^{2+}$	-0.2957	-0.0477	0.2480	-0.1717	0.1240	0.1189
[H ₂ Cit] $^{-}$	-0.1797	-0.0429	0.1368	-0.1113	0.0684	0.0906
[H ₂ NTA] $^{-}$	-0.1782	-0.0434	0.1348	-0.1108	0.0674	0.0911
[H ₂ EDTA] $^{2-}$	-0.1631	-0.0392	0.1239	-0.1012	0.0620	0.0826

The three intramolecular parameters of μ , η and ω are only related to the characteristics of an isolated molecule. In contrast, another parameter, namely charge transfer (ΔN) calculated using Equation (4) [32,47], will further contribute to reveal inherent the characteristics of the adsorption process.

$$\Delta N = \frac{(E_{\text{HOMO}}^B + E_{\text{LUMO}}^B - E_{\text{HOMO}}^A - E_{\text{LUMO}}^A)}{2(E_{\text{LUMO}}^A + E_{\text{LUMO}}^B - E_{\text{HOMO}}^A - E_{\text{HOMO}}^B)} \quad (4)$$

where the A and B superscripts are used to mark the species A and B . If $\Delta N < 0$, we can confirm that A and B serve as the electron donor and electron acceptor, respectively. Furthermore, the higher absolute value of ΔN will suggest the stronger interaction between two molecules [32,47]. The amounts of calculated charge transfer between the three cations (Ni(II), Pb(II) and Ca(II)) and the [EDTMPA-TBOT] $^{7-}$ ligand and those between Ni(II) and three complexing reagents (citrate, NTA and EDTA) are listed in Table 2. The negative ΔN indicates that Ni(II), Pb(II) and Ca(II) serve as electrophiles, while the [EDTMPA-TBOT] $^{7-}$ ligand and three complexing reagents act as nucleophiles. The calculated ΔN between Ni(II) and the [EDTMPA-TBOT] $^{7-}$ ligand ($\Delta N_{[\text{EDTMPA-TBOT}]^{7-} \rightarrow \text{Ni(II)}}$) is slightly lower than $\Delta N_{[\text{EDTMPA-TBOT}]^{7-} \rightarrow \text{Pb(II)}}$, but is much larger than $\Delta N_{[\text{EDTMPA-TBOT}]^{7-} \rightarrow \text{Ca(II)}}$, which indicates that the EDTMPA-TBOT/PVDF chelating membrane shows a strong affinity to Pb(II), followed by Ni(II) and lastly by Ca(II). The interference of Pb(II) on Ni(II) adsorption is more notable than that of Ca(II). In comparison with the value of $\Delta N_{[\text{EDTMPA-TBOT}]^{7-} \rightarrow \text{Ni(II)}}$, the lower absolute values of $\Delta N_{[\text{citrate-2H}]^{-} \rightarrow \text{Ni(II)}}$, $\Delta N_{[\text{NTA-2H}]^{-} \rightarrow \text{Ni(II)}}$ and $\Delta N_{[\text{EDTA-2H}]^{2-} \rightarrow \text{Ni(II)}}$ suggest that these three coexisting complexing reagents show a smaller affinity to Ni(II) than the EDTMPA-TBOT/PVDF chelating membrane. In addition, EDTA shows a more negative effect on the Ni(II) uptake than citrate and NTA.

Table 2. ΔN between the [EDTMPA-TBOT] $^{7-}$ ligand and Ni(II), Pb(II) and Ca(II) and that between Ni(II) and citrate, NTA and EDTA.

Reactant	[Ni(II)(H ₂ O) ₆] $^{2+}$	[Pb(II)(H ₂ O) ₂] $^{2+}$	[Ca(II)(H ₂ O) ₈] $^{2+}$
[EDTMPA-TBOT] $^{7-}$	-0.5560	-0.5621	-0.2375
[H ₂ Cit] $^{-}$	-0.3453	-	-
[H ₂ NTA] $^{-}$	-0.3500	-	-
[H ₂ EDTA] $^{2-}$	-0.4054	-	-

3.4.3. Complexing Sites of the EDTMPA-TBOT Ligand

As illustrated in Figure 7a, the chelating membrane will provide thirteen complexing sites: N₁, N₄, O₇, O₈, O₁₁, O₁₅, O₁₆, O₁₉, O₂₀, O₃₃, O₃₄, O₃₅ and O₃₆. Conventionally, Ni(II) will be complexed in the form of the six-coordinated configuration [39]. In addition, taking into account the nucleophilic characteristics of these complexing sites and the stability of the [Ni(II)-(EDTMPA-TBOT)] $^{5-}$ configuration, three configurations in correlation with the complexing sites of the EDTMPA-TBOT ligand were chosen (shown in Figure 8), and they are shown as follows: [Ni(II)-(O₃₃-O₁₅-O₁₆-O₇-O₁₉-O₃₆)] $^{5-}$,

$[\text{Ni}(\text{II})-(\text{O}_{33}-\text{O}_{15}-\text{O}_7-\text{O}_{19}-\text{O}_{36}-\text{O}_{34})]^{5-}$ and $[\text{Ni}(\text{II})-(\text{N}_1-\text{N}_4-\text{O}_{33}-\text{O}_{15}-\text{O}_7-\text{O}_{36})]^{5-}$. For the purpose of simple illustration, the above three complexes are denoted as $[\text{Ni}(\text{II})-(\text{EDTMPA-TBOT})]^{5-}$ -1, $[\text{Ni}(\text{II})-(\text{EDTMPA-TBOT})]^{5-}$ -2 and $[\text{Ni}(\text{II})-(\text{EDTMPA-TBOT})]^{5-}$ -3. As shown in Figure 8a, the bond lengths of Ni(II)-O₁₉ (3.545 Å) and Ni(II)-O₃₃ (3.022 Å) exceed 3.0 Å, indicating that the coordinating interactions between Ni(II) and O₁₉, O₃₃ cannot take place. The $[\text{Ni}(\text{II})-(\text{EDTMPA-TBOT})]^{5-}$ -1 complex will exist in the form of the four-coordinated conformation. Similarly, the length of the Ni(II)-O₃₆ bond in the $[\text{Ni}(\text{II})-(\text{EDTMPA-TBOT})]^{5-}$ -2 complex is 3.535 Å (shown in Figure 8b), so the $[\text{Ni}(\text{II})-(\text{EDTMPA-TBOT})]^{5-}$ -2 complex will be present with the form of the five-coordinated conformation [46]. However, the $[\text{Ni}(\text{II})-(\text{EDTMPA-TBOT})]^{5-}$ -3 complex can exist in a stable form of the six-coordinated conformation (presented in Figure 8c).

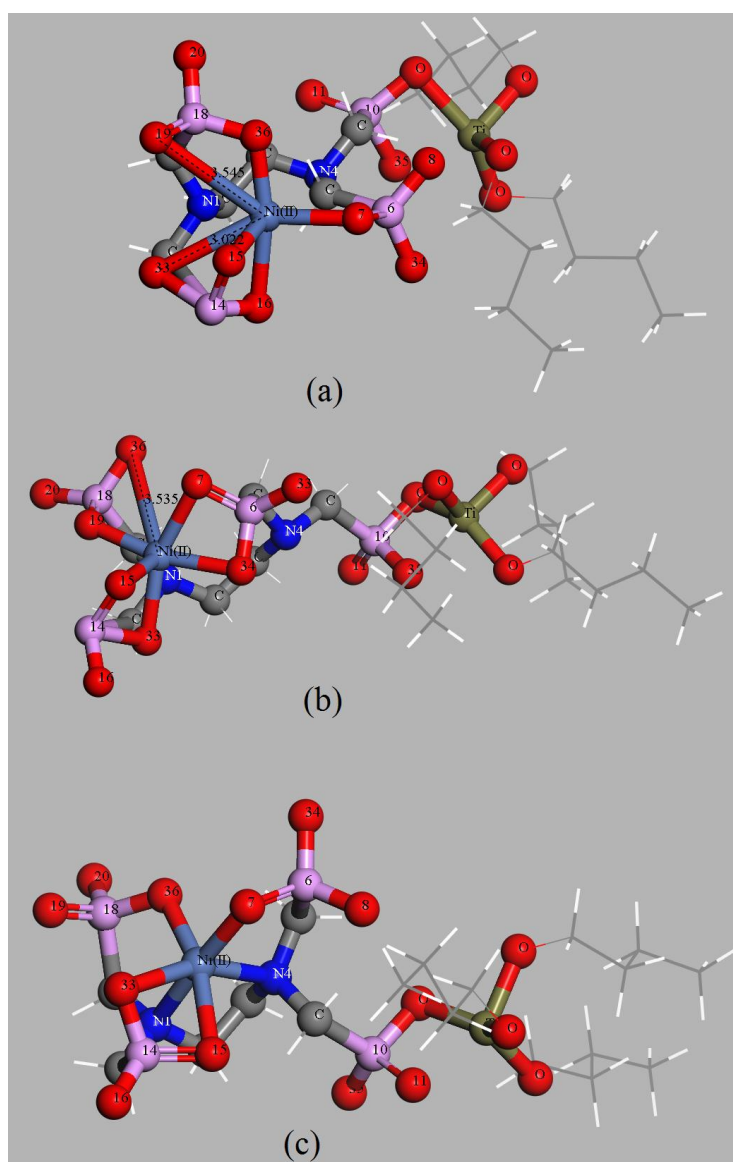


Figure 8. Optimized structures of the $[\text{Ni}(\text{II})-(\text{EDTMPA-TBOT})]^{5-}$ -1, $[\text{Ni}(\text{II})-(\text{EDTMPA-TBOT})]^{5-}$ -2 and $[\text{Ni}(\text{II})-(\text{EDTMPA-TBOT})]^{5-}$ -3 complexes with the numbered atoms: numbered atoms are denoted as follows: (a) $[\text{Ni}(\text{II})-(\text{EDTMPA-TBOT})]^{5-}$ -1 (7, 8, 11, 15, 16, 19, 20, 33–36, oxygen; 6, 10, 14, 18, phosphorus); (b) $[\text{Ni}(\text{II})-(\text{EDTMPA-TBOT})]^{5-}$ -2 (7, 8, 11, 15, 16, 19, 20, 33–36, oxygen; 6, 10, 14, 18, phosphorus); (c) $[\text{Ni}(\text{II})-(\text{EDTMPA-TBOT})]^{5-}$ -3 (7, 8, 11, 15, 16, 19, 20, 33–36, oxygen; 6, 10, 14, 18, phosphorus).

The adsorption energy (ΔE_{ads}) at 298 K obtained from Equation (5) can be valuable for elucidating the stability of complexing geometries [39,46].

$$\Delta E_{\text{ads}} = \Sigma E(\text{product}) - \Sigma E(\text{reactant}) \quad (5)$$

where $E(X)$ is the computed total energy of species (X) with respect to the COSMO effect. The calculated ΔE_{ads} for the above three complexes are -9092.55 , -9092.24 and -9092.91 kJ/mol. The $[\text{Ni}(\text{II})-(\text{EDTMPA-TBOT})]^{5-}$ complex has a minimum ΔE_{ads} , so this complex is more stable than the other two geometries. Therefore, the complex derived from the chelating interaction between Ni(II) and the membrane will be presented as the form of $[\text{Ni}(\text{II})-(\text{EDTMPA-TBOT})]^{5-}$.

When the EDTMPA-TBOT/PVDF chelating membrane absorbed Ni(II) with the coexistence of Ca(II) and Pb(II) cations and citrate, NTA and EDTA complexing reagents, the optimized geometries accompanied by minimum energies of the $[\text{Ca}(\text{II})-(\text{EDTMPA-TBOT})]^{5-}$, $[\text{Pb}(\text{II})-(\text{EDTMPA-TBOT})]^{5-}$, $[\text{Ni}(\text{II})-\text{citrate}]^+$, $[\text{Ni}(\text{II})-\text{NTA}]^+$ and $[\text{Ni}(\text{II})-\text{EDTA}]^0$ complexes are displayed in Figures 9 and 10. $[\text{Pb}(\text{II})-(\text{EDTMPA-TBOT})]^{5-}$ and $[\text{Ni}(\text{II})-\text{EDTA}]^0$ will be present in the six-coordinated conformations, while $[\text{Ni}(\text{II})-\text{NTA}]^+$ is the form of the four-coordinated conformation and $[\text{Ni}(\text{II})-\text{citrate}]^+$ a three-coordinated conformation. In addition, for the $[\text{Ca}(\text{II})-(\text{EDTMPA-TBOT})]^{5-}$ complex, the length of the Ca(II)-O₁₅ bond is 3.864 Å (Figure 9a), indicating the nonexistence of bonding interaction between Ca(II) and the O₁₅ atom. In this respect, the Ca(II)-[EDTMPA-TBOT]⁷⁻ complexes in the forms of the seven-coordinated conformation can be manifested.

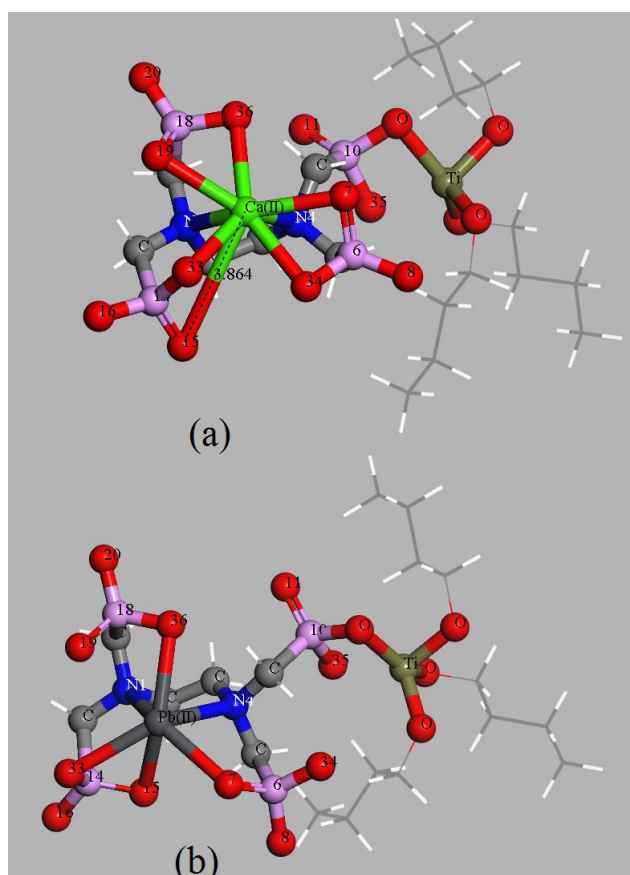


Figure 9. Optimized structures of $[\text{Ca}(\text{II})-(\text{EDTMPA-TBOT})]^{5-}$ and $[\text{Pb}(\text{II})-(\text{EDTMPA-TBOT})]^{5-}$ complexes with the numbered atoms: numbered atoms are denoted as follows: (a) $[\text{Ca}(\text{II})-(\text{EDTMPA-TBOT})]^{5-}$ (7, 8, 11, 15, 16, 19, 20, 33–36, oxygen; 6, 10, 14, 18, phosphorus); (b) $[\text{Pb}(\text{II})-(\text{EDTMPA-TBOT})]^{5-}$ (7, 8, 11, 15, 16, 19, 20, 33–36, oxygen; 6, 10, 14, 18, phosphorus).

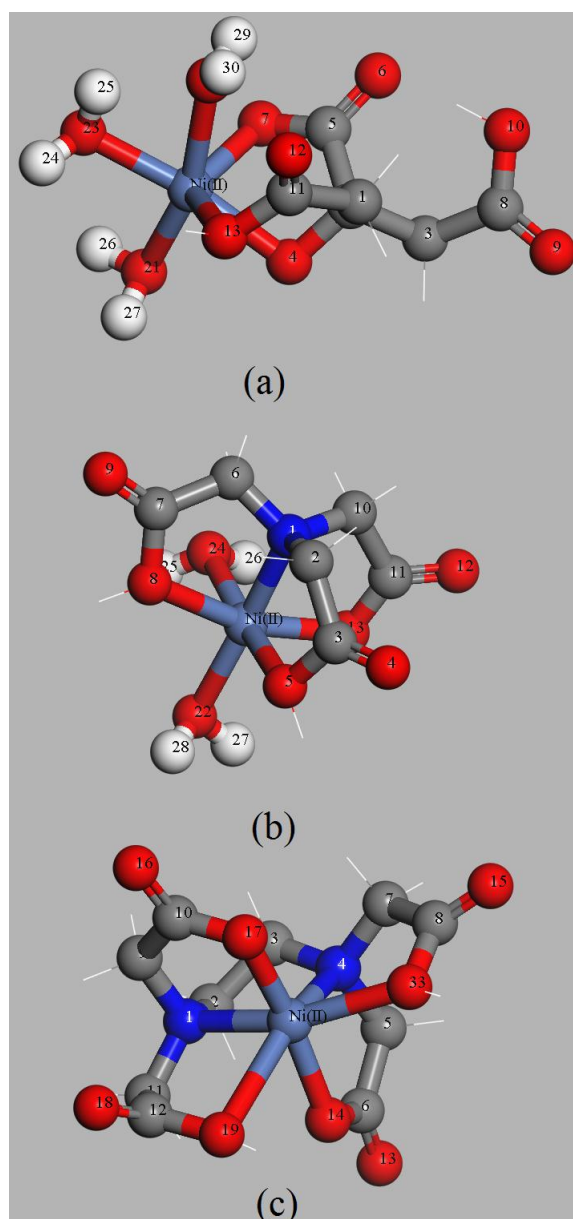


Figure 10. Optimized structures of $[\text{Ni}(\text{II})\text{-citrate}]^+$, $[\text{Ni}(\text{II})\text{-NTA}]^+$ and $[\text{Ni}(\text{II})\text{-EDTA}]^0$ complexes with the numbered atoms: numbered atoms are denoted as follows: (a) $[\text{Ni}(\text{II})\text{-citrate}]^+$ (24–27, 29, 30, hydrogen; 1–3, 5, 8, 11, carbon; 4, 6, 7, 9, 10, 12, 13, 21, 23, 28, oxygen); (b) $[\text{Ni}(\text{II})\text{-NTA}]^+$ (25–28, hydrogen; 2, 3, 6, 7, 10, 11, carbon; 4, 5, 8, 9, 12, 13, 22, 24, oxygen; 1, nitrogen); (c) $[\text{Ni}(\text{II})\text{-EDTA}]^0$ (2, 3, 5–12, carbon; 13–19, 33, oxygen; 1, 4, nitrogen).

3.4.4. Analyses of the Adsorption Energy and the Gibbs Free Energy of Adsorption

The Gibbs free energy of adsorption (ΔG_{ads}) at 298 K defined by Equation (6) was used to reveal the available formation of metal-based complexes; where $G(X)$ is the calculated temperature-corrected free energy of species (X) at 298 K [39,46] and ΔE_{ads} is already depicted by Equation (5).

$$\Delta G_{\text{ads}} = \Delta E_{\text{ads}} + (\Sigma G(\text{product}) - \Sigma G(\text{reactant})) \quad (6)$$

The calculated ΔE_{ads} and ΔG_{ads} of Ni(II)-, Pb(II)- and Ca(II)-(EDTMPA-TBOT) $^{7-}$ complexes and those of Ni(II)-citrate, -NTA and -EDTA complexes are tabulated in Table 3. ΔG_{ads} with a negative value reflects the spontaneous characteristic of Ni(II) adsorption. ΔE_{ads} of the three

kinds of metal-[EDTMPA-TBOT]⁷⁻ complexes is in the order of [Pb(II)-(EDTMPA-TBOT)]⁵⁻ < [Ni(II)-(EDTMPA-TBOT)]⁵⁻ < [Ca(II)-(EDTMPA-TBOT)]⁵⁻, indicating that the complexation ability of the EDTMPA-TBOT/PVDF chelating membrane toward three metal ions follows the sequence: Pb(II) > Ni(II) > Ca(II). This result is consistent with the experimental analysis. The chelating membrane exhibits a more excellent affinity to Pb(II) and Ni(II) than Ca(II), and thus, Pb(II) will remarkably interfere with the uptake of Ni(II). In addition, it can be deduced that the fabricated chelating membrane can be competent for removing heavy metals with a high biotoxicity from the aqueous solution.

Table 3. Calculated values of ΔE_{ads} and ΔG_{ads} for the metal-based complexes.

Reactant	$\Delta E_{\text{ads}}/(\text{kJ/mol})$	$\Delta G_{\text{ads}}/(\text{kJ/mol})$
[Ni(II)-(EDTMPA-TBOT)] ⁵⁻	-58.30	-114.20
[Pb(II)-(EDTMPA-TBOT)] ⁵⁻	-112.47	-117.85
[Ca(II)-(EDTMPA-TBOT)] ⁵⁻	-12.88	-91.97
[Ni(II)-citrate] ⁺	16.88	-24.71
[Ni(II)-NTA] ⁺	8.07	-3.55
[Ni(II)-EDTA] ⁰	-6.41	-59.51

The coexisting citrate, NTA and EDTA can form stable complexes with Ni(II). Considering the ΔE_{ads} value between Ni(II) and these, it can be concluded that the detrimental influence of the three complexing reagents follows the sequence of EDTA > NTA > citrate. However, the abilities of these three complexing reagents with respect to the uptake of Ni(II) are smaller than that of the EDTMPA-TBOT/PVDF chelating membrane. Based on the result of this research, with the coexistence of complexing reagents, the fabricated EDTMPA-TBOT/PVDF chelating membrane is still applicable for the recovery of Ni(II) from aqueous solution.

4. Conclusions

The fabricated EDTMPA-TBOT/PVDF chelating membrane was employed for the removal of Ni(II) from aqueous solutions. Batch adsorption experiments in conjunction with DFT calculations were employed to evaluate the adsorption characteristics of the chelating membrane toward Ni(II) in the presence of Ca(II), Pb(II), citrate, NTA and EDTA. The obtained conclusions are summarized as follows:

- (1) The combination of DFT simulations and the adsorption experiments is suitable for evaluating the adsorption process between Ni(II) and the EDTMPA-TBOT/PVDF chelating membrane.
- (2) The coexistent Pb(II) shows a stronger interferential effect on Ni(II) uptake than Ca(II). Furthermore, the disturbance of EDTA on the Ni(II) uptake of the EDTMPA-TBOT/PVDF membrane is more remarkable than those of NTA and citrate.
- (3) The large absolute value of charge transfer, the negative values of adsorption energy and Gibbs free energy of adsorption for the [Ni(II)-(EDTMPA-TBOT)]⁵⁻ and [Pb(II)-(EDTMPA-TBOT)]⁵⁻ complexes suggests that the fabricated EDTMPA-TBOT/PVDF chelating membrane will be qualified for the removal heavy metals with a high biotoxicity from the aqueous solution.

Acknowledgments: This work was funded by the Scientific Research Foundation of the Hebei Higher Education Institutions of China (Grant No. ZD2015120) and the Hebei Provincial Natural Science Foundation of China (Grant No. B2016203012).

Author Contributions: Xiuli Wang performed the DFT simulations and prepared the manuscript. Laizhou Song designed this work and gave the guidance for DFT simulations. Caili Tian contributed the measurement of FE-SEM and EDS. Jun He and Shuaijie Wang analyzed the data and reviewed the manuscript. Jinbo Wang and Chunyu Li performed the experiments and the measurement of FTIR. All authors read and approved the manuscript.

Conflicts of Interest: All authors declare that there is no any conflict of interest.

References

1. Cempel, M.; Nikel, G. Nickel: A review of its sources and environmental toxicology. *Pol. J. Environ. Stud.* **2006**, *15*, 375–382.
2. Waalkes, M.P.; Liu, J.; Kasprzak, K.S.; Diwan, B.A. Minimal influence of metallothionein over-expression on nickel carcinogenesis in mice. *Toxicol. Lett.* **2004**, *153*, 357–364. [[CrossRef](#)] [[PubMed](#)]
3. Wang, L.; Liu, R.T.; Teng, Y. Study on the toxic interactions of Ni²⁺ with DNA using neutral red dye as a fluorescence probe. *J. Lumin.* **2011**, *131*, 705–709. [[CrossRef](#)]
4. Song, L.Z.; He, J.; Wang, X.L.; Wang, T. Thermodynamic and kinetic investigations of a chelating membrane bearing polyaminecarboxylate groups towards Ni(II). *Toxicol. Environ. Chem.* **2012**, *94*, 1902–1915. [[CrossRef](#)]
5. Shih, Y.J.; Lin, C.P.; Huang, Y.H. Application of Fered-Fenton and chemical precipitation process for the treatment of electroless nickel plating wastewater. *Sep. Purif. Technol.* **2013**, *104*, 100–105. [[CrossRef](#)]
6. Franco, P.E.; Veit, M.T.; Borba, C.E.; Gonçalves, G.D.C.; Fagundes-Klen, M.R.; Bergamasco, R.; Silva, E.A.D.; Suzaki, P.Y.R. Nickel(II) and zinc(II) removal using Amberlite IR-120 resin: Ion exchange equilibrium and kinetics. *Chem. Eng. J.* **2013**, *221*, 426–435. [[CrossRef](#)]
7. Hanif, M.A.; Nadeem, R.; Bhatti, H.N.; Ahmad, N.R.; Ansari, T.M. Ni(II) biosorption by *Cassia fistula* (Golden Shower) biomass. *J. Hazard. Mater.* **2007**, *139*, 345–355. [[CrossRef](#)] [[PubMed](#)]
8. Silva, J.E.; Paiva, A.P.; Soares, D.; Labrincha, A.; Castro, F. Solvent extraction applied to the recovery of heavy metals from galvanic sludge. *J. Hazard. Mater.* **2005**, *120*, 113–118. [[CrossRef](#)] [[PubMed](#)]
9. Hoseinian, F.S.; Irannajad, M.; Nooshabadi, A.J. Ion flotation for removal of Ni(II) and Zn(II) ions from wastewaters. *Int. J. Miner. Process.* **2015**, *143*, 131–137. [[CrossRef](#)]
10. Dermentzis, K.; Christoforidis, A.; Valsamidou, E. Removal of nickel, copper, zinc and chromium from synthetic and industrial wastewater by electrocoagulation. *Int. J. Environ. Sci.* **2011**, *1*, 697–710.
11. Gupta, B.S.; Curran, M.; Hasan, S.; Ghosh, T.K. Adsorption characteristics of Cu and Ni on Irish peat moss. *J. Environ. Manag.* **2009**, *90*, 954–960. [[CrossRef](#)] [[PubMed](#)]
12. Zhao, F.P.; Tang, W.Z.; Zhao, D.B.; Meng, Y.; Yin, D.L.; Sillanpää, M. Adsorption kinetics, isotherms and mechanisms of Cd(II), Pb(II), Co(II) and Ni(II) by a modified magnetic polyacrylamide microcomposite adsorbent. *J. Water Process Eng.* **2014**, *4*, 47–57. [[CrossRef](#)]
13. Nabarlantz, D.; Celis, J.D.; Bonelli, P.; Cukierman, A.L. Batch and dynamic sorption of Ni(II) ions by activated carbon based on a native lignocellulosic precursor. *J. Environ. Manag.* **2012**, *97*, 109–115. [[CrossRef](#)] [[PubMed](#)]
14. Mohammad, A.W.; Othaman, R.; Hilal, N. Potential use of nanofiltration membranes in treatment of industrial wastewater from Ni-P electroless plating. *Desalination* **2004**, *168*, 241–252. [[CrossRef](#)]
15. Song, L.Z.; Yang, M.; Fu, J.; Lu, P.P.; Wang, X.L.; He, J. Adsorption performance of APTMS-DTPA/PVDF chelating membrane toward Ni(II) with the presence of Ca(II), NH₄⁺, lactic acid, and citric acid. *Desalin. Water Treat.* **2015**, *53*, 158–170. [[CrossRef](#)]
16. Arthanareeswaran, G.; Thanikaivelan, P.; Raguime, J.A.; Raajenthiren, M.; Mohan, D. Metal ion separation and protein removal from aqueous solutions using modified cellulose acetate membranes: Role of polymeric additives. *Sep. Purif. Technol.* **2007**, *55*, 8–15. [[CrossRef](#)]
17. Dermentzis, K. Removal of nickel from electroplating rinse waters using electrostatic shielding electro dialysis/electrodeionization. *J. Hazard. Mater.* **2010**, *173*, 647–652. [[CrossRef](#)] [[PubMed](#)]
18. Kumbasar, R.A.; Kasap, S. Selective separation of nickel from cobalt in ammoniacal solutions by emulsion type liquid membranes using 8-hydroxyquinoline (8-HQ) as mobile carrier. *Hydrometallurgy* **2009**, *95*, 121–126. [[CrossRef](#)]
19. Barakat, M.A.; Schmidt, E. Polymer-enhanced ultrafiltration process for heavy metals removal from industrial wastewater. *Desalination* **2010**, *256*, 90–93. [[CrossRef](#)]
20. Richards, L.A.; Richards, B.S.; Schafer, A.I. Renewable energy powered membrane technology: Salt and inorganic contaminant removal by nanofiltration/reverse osmosis. *J. Membr. Sci.* **2011**, *369*, 188–195. [[CrossRef](#)]
21. Wang, C.-C.; Wang, C.-C. Adsorption characteristics of metal complexes by chelated copolymers with amino group. *React. Funct. Polym.* **2006**, *66*, 343–356. [[CrossRef](#)]
22. Vetrivelvi, V.; Santhi, R.J. Redox polymer as an adsorbent for the removal of chromium(VI) and lead(II) from the tannery effluents. *Water Res. Ind.* **2015**, *10*, 39–52. [[CrossRef](#)]
23. Long, H.; Wu, P.X.; Zhu, N.W. Evaluation of Cs⁺ removal from aqueous solution by adsorption on ethylamine-modified montmorillonite. *Chem. Eng. J.* **2013**, *225*, 237–244. [[CrossRef](#)]

24. Deng, S.B.; Ting, Y.P. Characterization of PEI-modified biomass and biosorption of Cu(II), Pb(II) and Ni(II). *Water Res.* **2005**, *39*, 2167–2177. [[CrossRef](#)] [[PubMed](#)]
25. Yoo, H.; Kwak, S.Y. Surface functionalization of PTFE membranes with hyperbranched poly (amidoamine) for the removal of Cu²⁺ ions from aqueous solution. *J. Membr. Sci.* **2013**, *448*, 125–134. [[CrossRef](#)]
26. Adewuyi, A.; Pereira, F.V. Nitrilotriacetic acid functionalized *Adansonia digitata* biosorbent: Preparation, characterization and sorption of Pb(II) and Cu(II) pollutants from aqueous solution. *J. Adv. Res.* **2016**, *7*, 947–959. [[CrossRef](#)] [[PubMed](#)]
27. Baraka, A.; Hall, P.J.; Heslop, M.J. Preparation and characterization of melamine–formaldehyde–DTPA chelating resin and its use as an adsorbent for heavy metals removal from wastewater. *React. Funct. Polym.* **2007**, *67*, 585–600. [[CrossRef](#)]
28. Zhao, X.D.; Song, L.Z.; Fu, J.; Tang, P.; Liu, F. Adsorption characteristics of Ni(II) onto MA–DTPA/PVDF chelating membrane. *J. Hazard. Mater.* **2011**, *189*, 732–740. [[CrossRef](#)] [[PubMed](#)]
29. Ma, T.Y.; Zhang, X.J.; Yuan, Z.Y. Hierarchically meso-/macroporous titanium tetraphosphonate materials: Synthesis, photocatalytic activity and heavy metal ion adsorption. *Microporous Mesoporous Mater.* **2009**, *123*, 234–242. [[CrossRef](#)]
30. Repo, E.; Warchoń, J.K.; Bhatnagar, A.; Sillanpää, M. Heavy metals adsorption by novel EDTA-modified chitosan-silica hybrid materials. *J. Colloid Interface Sci.* **2011**, *358*, 261–267. [[CrossRef](#)] [[PubMed](#)]
31. Flores-Holguín, N.; Aguilar-Elguézabal, A.; Rodríguez-Valdez, L.M.; Glossman-Mitnik, D. Theoretical study of chemical reactivity of the main species in the α -pinene isomerization reaction. *J. Mol. Struct. Theochem.* **2008**, *854*, 81–88. [[CrossRef](#)]
32. Srivastava, A.; Rawat, P.; Tandon, P.; Singh, R.N. A computational study on conformational geometries, chemical reactivity and inhibitor property of an alkaloid bicuculline with γ -aminobutyric acid (GABA) by DFT. *Comput. Theor. Chem.* **2012**, *993*, 80–89. [[CrossRef](#)]
33. Yeh, C.-W.; Chen, J.-D. Role of ligand conformation in the structural diversity of divalent complexes containing phosphinic amide ligand. *Inorg. Chem. Commun.* **2011**, *14*, 1212–1216. [[CrossRef](#)]
34. Romanowski, Z.; Kempisty, P.; Sakowski, K.; Krukowski, S. Polarization analysis and Density Functional Theory (DFT) simulations of the electric field in InN/GaN multiple quantum wells (MQWs). *J. Phys. Chem. C* **2009**, *114*, 14410–14416. [[CrossRef](#)]
35. Savizi, I.S.P.; Janik, M.J. Acetate and phosphate anion adsorption linear sweep voltammograms simulated using density functional theory. *Electrochim. Acta* **2011**, *56*, 3996–4006. [[CrossRef](#)]
36. Rahnemaie, R.; Hiemstra, T.; Riemsdijk, W.H. Carbonate adsorption on goethite in competition with phosphate. *J. Colloid Interface Sci.* **2007**, *315*, 415–425. [[CrossRef](#)] [[PubMed](#)]
37. Acelas, N.Y.; Mejia, S.M.; Mondragón, F.; Flórez, E. Density functional theory characterization of phosphate and sulfate adsorption on Fe-(hydr)oxide: Reactivity, pH effect, estimation of Gibbs free energies, and topological analysis of hydrogen bonds. *Comput. Theor. Chem.* **2013**, *1005*, 16–24. [[CrossRef](#)]
38. Ren, X.M.; Yang, S.T.; Tan, X.L.; Chen, C.L.; Sheng, G.D.; Wang, X.K. Mutual effects of copper and phosphate on their interaction with γ -Al₂O₃: Combined batch macroscopic experiments with DFT calculations. *J. Hazard. Mater.* **2012**, *237–238*, 199–208. [[CrossRef](#)] [[PubMed](#)]
39. Song, L.Z.; Zhao, X.D.; Fu, J.; Wang, X.L.; Sheng, Y.P.; Liu, X.W. DFT investigation of Ni(II) adsorption onto MA-DTPA/PVDF chelating membrane in the presence of coexistent cations and organic acids. *J. Hazard. Mater.* **2012**, *199–200*, 433–439. [[CrossRef](#)] [[PubMed](#)]
40. Zhao, C.S.; Zhou, X.S.; Yue, Y.L. Determination of pore size and pore size distribution on the surface of hollow-fiber filtration membranes: A review of methods. *Desalination* **2000**, *129*, 107–123. [[CrossRef](#)]
41. Wang, X.L.; Song, L.Z.; Yang, F.F.; He, J. Investigation of phosphate adsorption by a polyethersulfone-type affinity membrane using experimental and DFT methods. *Desalin. Water Treat.* **2016**, *57*, 25036–25056. [[CrossRef](#)]
42. Chen, C.; Shen, C.H.; Kong, G.J.; Gao, S.J. High temperature proton exchange membranes prepared from epoxyhexylethyltrimethoxysilane and amino trimethylene phosphonic acid as anhydrous proton conductors. *Mater. Chem. Phys.* **2013**, *140*, 24–30. [[CrossRef](#)]
43. Xu, J.F.; Wu, X.Y.; Fu, G.T.; Liu, X.Y.; Chen, Y.; Zhou, Y.M.; Tang, Y.W.; Lu, T.H. Fabrication of phosphonate functionalized platinum nanoclusters and their application in hydrogen peroxide sensing in the presence of oxygen. *Electrochim. Acta* **2012**, *80*, 233–239. [[CrossRef](#)]

44. Ma, T.Y.; Li, H.; Tang, A.N.; Yuan, Z.Y. Ordered, mesoporous metal phosphonate materials with microporous crystalline walls for selective separation techniques. *Small* **2011**, *7*, 1827–1837. [[CrossRef](#)] [[PubMed](#)]
45. Ferrah, N.; Abderrahim, O.; Didi, M.A.; Villemin, D. Removal of copper ions from aqueous solutions by a new sorbent: Polyethyleneiminemethylene phosphonic acid. *Desalination* **2011**, *269*, 17–24. [[CrossRef](#)]
46. Song, L.Z.; Zhao, R.F.; Yun, D.D.; Lu, P.P.; He, J.; Wang, X.L. Influence of Co(II), Ni(II), tartrate, and ethylenediaminetetraacetic acid on Cu(II) adsorption onto a polyvinylidene fluoride-based chelating membrane. *Toxicol. Environ. Chem.* **2014**, *96*, 362–378. [[CrossRef](#)]
47. Kumar, V.; Jain, G.; Kishor, S.; Ramaniah, L.M. Chemical reactivity analysis of some alkylating drug molecules—A density functional theory approach. *Comput. Theor. Chem.* **2011**, *968*, 18–25. [[CrossRef](#)]



© 2017 by the authors; licensee MDPI, Basel, Switzerland. This article is an open access article distributed under the terms and conditions of the Creative Commons Attribution (CC BY) license (<http://creativecommons.org/licenses/by/4.0/>).